This paper is a declared work of the U. S. Government and is not subject to copyright protection in the United States.
PAPER AAS 93-571

TOPEX/POSEIDON ORBIT ACQUISITION MANEUVER SEQUENCE

Ramachandra S. Bhat
Bruce E. Shapiro
Raymond B. Frauenholz

Jet Propulsion Laboratory
California Institute of Technology
Pasadena, California

AAS/AIAA Astrodynamics Specialist Conference

VICTORIA, B.C., CANADA AUGUST 16-19, 1993

AAS Publications Office, P.O. Box 28130, San Diego, CA 92198

This paper is a declared work of the U. S. Government and is not subject to copyright protection in the United States.

AAS 93-571

TOPEX/POSEIDON ORBIT ACQUISITION MANEUVER SEQUENCE*

Ramachandra S. Bhat†, Bruce E. Shapiro‡, and Raymond. B. Frauenholz**
Jet Propulsion Laboratory, California Institute of Technology, Pasadena, CA, 91109

A sequence of six maneuvers was implemented over a 42-day period following the launch of the TOPEX/POSEIDON satellite on August 10, 1992 to acquire an orbit compatible with oceanographic data acquisition requirements as soon as possible. These maneuvers raised and circularized the orbit, removed inclination errors imparted by the launch vehicle, acquired frozen orbit conditions, and synchronized the ground track with an exact repeat reference grid which overflies two verification sites. Initial maneuver sequence design incorporated the best pre-launch execution error estimates. Observed maneuver performance characteristics were incorporated into the error model and the remaining sequence was redesigned after each maneuver. Accurate maneuver performance evaluation used a newly developed technique based on the mean elements. Maneuver magnitudes were determined to an accuracy of better than 0.2 mm/s and precise thruster recalibration was possible after each maneuver. Maneuver sequence design was adaptable to unexpected schedule changes and accommodated additional satellite operational health and welfare constraints and was coordinated with initial satellite startup and calibration procedures. A backup was designed for each maneuver to accommodate the possibility of operational delays, and was used for the first maneuver. The six-maneuver Orbit Acquisition Phase was successfully completed on September 21, 1992, providing a smooth transition to the Orbit Maintenance Phase.

INTRODUCTION

TOPEX/POSEIDON is a joint US/French†† mission designed to study global ocean circulation and its interaction with the atmosphere to better understand the Earth's climate.[1] This goal is accomplished utilizing a combination of satellite altimetry data and precision orbit determination to precisely determine ocean surface topography. To facilitate this process the satellite is maintained in a nearly circular, frozen orbit ($e \approx 0.000095$ and $\omega \approx 90°$) at an altitude of $\approx$1336 km and an inclination of $i \approx 66.04°$. This provides an exact repeat ground track every 127 revolutions ($\approx$9.9 days) and overflies two altimeter verification sites.[2] The satellite was launched by an Ariane 42P on August 10, 1992 and injected into a nearly circular $\approx$1322 km orbit with $i \approx$

---

* The work described in this paper was carried out by the Jet Propulsion Laboratory, California Institute of Technology, under contract with the National Aeronautics and Space Administration.

† Member Technical Staff, Navigation Systems Section.

‡ Member Technical Staff, Navigation Systems Section. Member AAS, Member AIAA.

** Technical Manager, Navigation Systems Section. Member AIAA.

†† The mission is jointly funded by the US National Aeronautics and Space Administration (NASA) and the French Centre National d'Etudes Spatiales (CNES).

66.08° at 23:27:05 UTC, approximately 19 min. 57 sec after liftoff. The injection orbit was biased to provided frequent opportunities for maneuver sequences which would phase smoothly into the reference ground track, as well as to avoid the possibility of a collision with the third stage of the launch vehicle. To begin timely altimeter data acquisition, mission objectives required that the operational orbit be acquired in the minimum practical amount of time.[3]

The satellite was built by the Fairchild Space Company (FS) under contract to the Jet Propulsion Laboratory (JPL). JPL is responsible for conducting all satellite mission operations including operational navigation. Operational orbit determination using radiometric data acquired via the NASA Tracking and Data Relay Satellite System (TDRSS) is provided[4] by the Flight Dynamics Facility (FDF) of NASA's Goddard Space Flight Center (GSFC). Early orbit determination solutions based upon Deep Space Network (DSN) tracking data were also provided. All satellite commands originate at the Payload Operations Control Center (POCC) which is located at JPL. While continuous interaction between all satellite operations teams is necessary to successfully execute any maneuver sequence, this paper is limited to the activities performed by the Navigation Team (NAVT). Other teams are responsible for command validation, sequencing, uplink, and verification.

This paper describes the design, implementation, and evaluation of the TOPEX/POSEIDON operational orbit acquisition maneuver sequence. The adaptive nature of the maneuver sequence design, which was able to easily accommodate schedule changes and additional satellite constraints, is presented. Finally, a brief description of the maneuver evaluation process is provided and the performance of each maneuver of the sequence is illustrated.

ORBIT REQUIREMENTS

The operational TOPEX/POSEIDON orbit is summarized in Table 1. This orbit was defined to produce a ground track which repeats after every 127 orbits (≈9.9 days) and overflies both verification sites in the absence of non-gravitational perturbations. The operational orbit is referred to as the *reference orbit* and the Keplerian elements describing this orbit are called the *reference elements*. The ascending node crossing longitudes of the reference orbit define the *reference grid*. The orbit acquisition maneuver sequence was designed with the reference elements and the reference grid as target parameters.

The operational orbit was initially designed to meet the scientific requirements with a semi-analytical trajectory program in the presence of a 17×17 truncation of the GEMT2 earth gravity field,[5,6] and was later refined[7] with a precision numerical integration using a 20×20 truncation of GEMT3.[8] The operational orbit is a nearly circular frozen orbit at an altitude of ≈1336 km and an inclination of i≈66.04°. The equatorial distance between two consecutive ascending nodes of the reference orbit is ≈3156 km and there are 10 reference tracks between any two consecutive equatorial ascending node crossings.

Early orbit determination solutions had epochs of separation (August 10, 1992 at 23:27:50 UTC) and were provided by the FDF approximately 4, 5.5, 7.5, 9, 20, and 36 hours after injection. The injection orbit was well established by the 20 hours (L+20) solution. The L+36 hour solution was used to design the initial maneuver sequence based on the achieved injection orbit. The expected and achieved mean orbital elements[9] at injection are also shown in Table 1. The achieved semi-major axis was ≈2.5 km less than expected. The mean apogee and perigee altitudes were 1326 km and 1319 km, respectively, placing the achieved injection orbit inside the operational orbit, as shown in Fig. 1. The nodal period was ≈18.5 secs less than that of the operational orbit, and the inclination 41.6 mdeg higher, requiring a plane change correction of ΔV≈5.2 m/s (Fig. 2). The ground track of the injection orbit had an eastward drift of ≈108.08

km/day with respect to the reference. This provided a synchronizing opportunity once every ≈2.9 days.

Table 1
Reference and injection mean orbital elements. Injection occurred at 23:27:50 UTC on Aug. 10, 1992.

Parameter	Expected Injection Orbit	Achieved Injection Orbit	Reference (Operational) Orbit	Required Parameter Change	Required ΔV
a, km	7703.056	7700.547	7714.429	13.882	6.4 m/s
$e \times 10^{-6}$	772	485	95	390	**
ω	6.4°	7.8	90.0°	82.2°	**
i*	66.0400°	66.0816°	66.0400°	0.0416	5.2 m/s
τ_N, sec	6730.83	6727.60	6745.75	18.15	

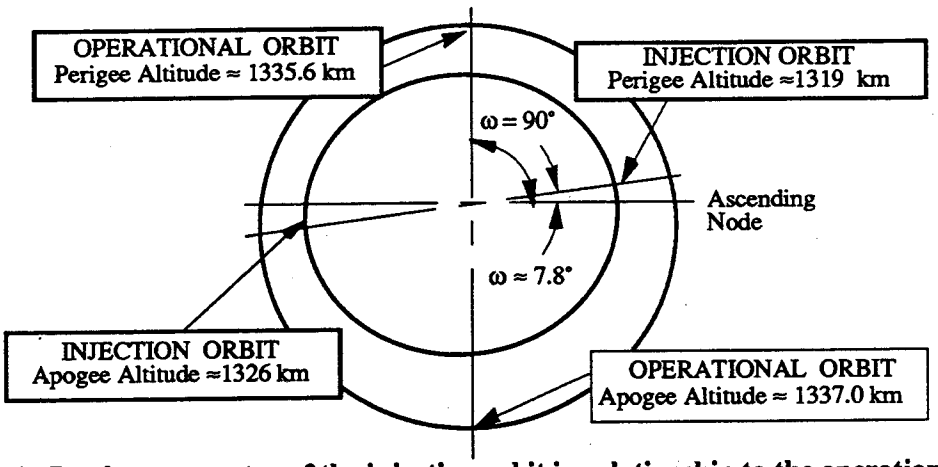

Figure 1. In-plane geometry of the injection orbit in relationship to the operational orbit.

The purpose of the orbit acquisition maneuver sequence was to acquire the operational orbit as quickly as possible, subject to all operational and satellite health and safety constraints, and provide a smooth transition to the orbit maintenance phase. Each maneuver in the sequence was individually targeted to an intermediate set of mean orbital parameters in such a way that the sequence of post-maneuver orbits converged on the operational orbit and the ground track was correctly phased. The first orbit of the 127-revolution ground track repetition cycle was defined to have an ascending node at 99.92° E longitude.[1] Individual orbits within a cycle are numbered consecutively starting at this node (rev. 1 through rev. 127). Successive cycles are numbered for reference purposes so that Cycle 1 was the first complete ≈9.9 day cycle starting with rev. 1 following acquisition of the operational orbit. Orbit maintenance maneuvers are required to be

* Gravity mean value. The gravity mean value is determined by eliminating all 3rd body periodic gravitational perturbations (i.e. luni-solar gravity) with periods shorter than 1000 days. The normal mean inclination varies about the gravity mean value due to these third body perturbations. Thus the gravity mean inclination was used as the target parameter.

** No special maneuvers were specifically required to change e and ω as these parameters were changed in conjunction with the Δa maneuvers.

performed at the transition between cycles (±1 orbit). The final maneuver of the acquisition sequence was designed so that the residual ground track drift rate would carry the ground track to eastern edge of the ±1 km wide control band on the date of the first schedule orbit maintenance maneuver. Consequently, the last few maneuvers of the sequence were progressively smaller in magnitude as the orbit was fine tuned.

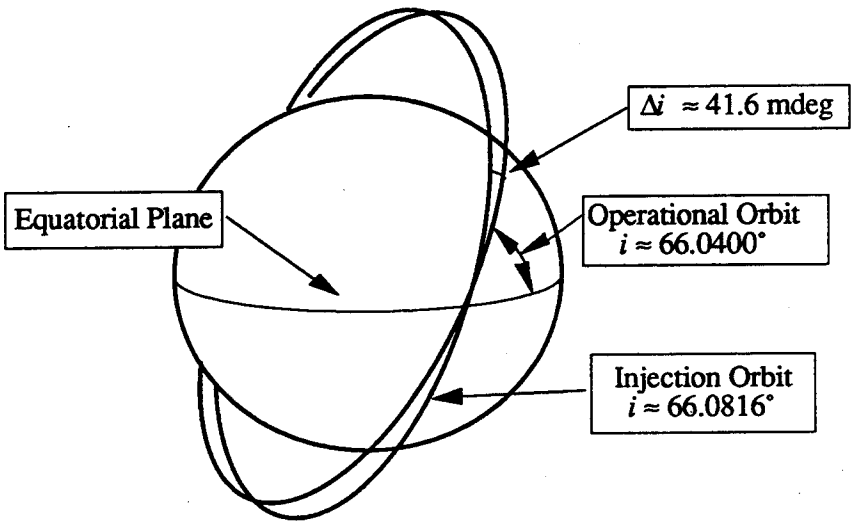

Figure 2. Injection and operational orbits.

SATELLITE CHARACTERISTICS

The TOPEX/POSEIDON satellite bus consists of a NASA standard Multi-mission Modular Spacecraft (MMS) modified to meet mission requirements and a TOPEX/POSEIDON-specific instrument module (see Fig. 5, below). Other noticeable features include a ≈2 meter steerable high-gain antenna used for TDRS communications, two omnidirectional DSN antennas, a global positioning system (GPS) demonstration antenna at the end of a 12-ft boom, and a dominant $28m^2$, continuously steerable 4-panel solar array. The seven payload instruments consist of four operational sensors (a dual frequency radar altimeter, a microwave radiometer, a laser-ranging retro-reflector array, and a DORIS dual Doppler tracking system receiver), two experimental sensors (a single-frequency solid-state radar altimeter and the GPS demonstration receiver), and a frequency reference unit.

The propulsion module (Fig. 3) is a mono-propellant hydrazine blow-down system consisting of twelve 1-N (0.2 lbf) and four 22-N (5-lbf) thrusters. It was designed to provide sufficient thrust and directional control to meet all orbit adjustment and maintenance maneuver requirements, including related attitude control. The propellant tank was fully loaded a few hours prior to launch to provide a total ΔV equivalent to ≈172 m/s. The system is capable of implementing maneuvers between 0.013 mm/s and 15 m/s.[3,10] The 22-N thrusters and four of the 1-N thrusters are mounted on the aft facing of the satellite. Large orbit adjustment maneuvers (>400 mm/sec) were performed using the 22-N thrusters. Smaller maneuvers (< 400 mm/sec), such as the final two maneuvers of the orbit acquisition sequence, were performed using four 1-N thrusters. Orbit maintenance maneuvers, which are much smaller, (typically < 10 mm/sec) use a single pair of 1-N thrusters.

The Center of Mass (CM) of the satellite does not coincide with the center of body coordinates due to the location of the solar panel as illustrated in Fig. 3. The orbit adjust thrusters were canted prior to the launch to align the thrust vector with the predicted CM. Each of these thrusters is oriented axially along the x-axis and individually canted to be aligned through the CM at the beginning of life when the propellant tanks are full. The remaining eight 1-N thrusters are mounted normal to the satellite x-axis to provide attitude control about any of the three body axes.

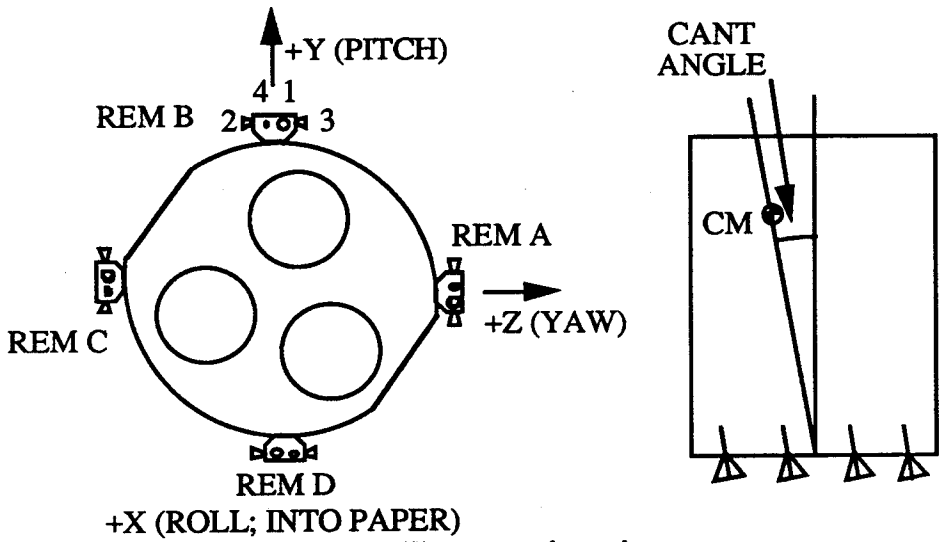

Figure 3. Thruster orientation.

Maneuver efficiency was expected to be less than 100% because of thruster duty cycling. Dynamic simulations[12] indicated that the worst-case maneuver efficiency using an *open loop firing pattern** (OLFP) would be ≈60%. Although it was decided not to use the OLFP to avoid large excitations, the observed duty cycle always exceeded 60% for large maneuvers and 85% for small maneuvers. Changes in the expected maneuver efficiency shift the centroid of the burn away from the planned time. The maneuver design was insensitive to moderate changes in the maneuver centroid time.[11]

The three-axis stabilized spacecraft utilizes nearly continuous sinusoidal yaw steering and solar array pitching for optimal solar-array pointing. In addition, the solar array normal is offset from the true sun line to control battery charging. To correctly orient the thrusters for maneuver execution, yaw steering must be temporarily suspended and the satellite slewed before and after the thrusters are fired. The yaw turn is accomplished using only reaction wheels. The turn duration varies depending on the initial yaw rate and turn angle (≈20 min to ≈70 min). Fig. 4 illustrates the "turn-burn-turn" sequence used to perform an orbit adjustment maneuver:

1. Suspend nominal attitude control and yaw steering.
2. Slew the satellite to the bias attitude which accounts for the cants of the thrusters and the desired thrust directions. In-plane maneuvers are performed with the thrust vector approximately aligned with the velocity vector, and purely out-of-plane maneuvers with the thrust vector approximately perpendicular to the plane of the orbit.

---

* With an OLFP, axial thrusters are off-pulsed to account for anticipated disturbance torques imparted by thruster/center-of-mass offsets. If the established pitch or yaw control limits are exceeded, orbit adjustment thrusters and the OLFP are disabled, and the 1-N thrusters are used to reestablish attitude control. The maneuver is resumed as soon as control limits are met.

3. For large maneuvers (requiring the 22-N thrusters), park the HGA.
4. For large maneuvers, rotate the solar array to a 90° or 270° pitch position.
5. Stop solar array pitching.
6. Execute the ΔV.
7. Reduce attitude rates induced by the ΔV thrusting.
8. Unwind the attitude.
9. Return the solar array to sun pointing.
10. Resume solar array pitching.
11. Return attitude control to normal mission mode.

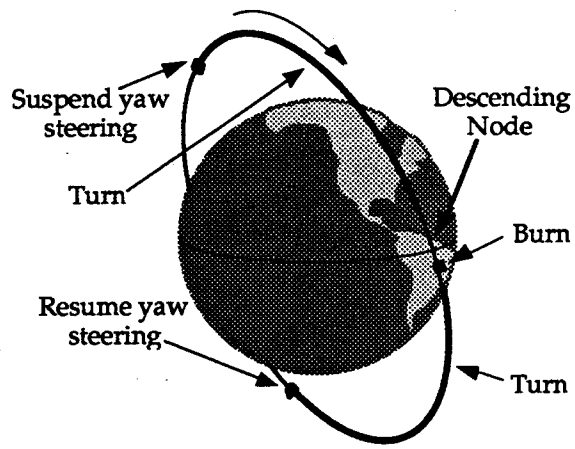

Figure 4. Maneuver turn-burn-turn sequence.

OPERATIONAL CONSTRAINTS

Operational constraints were initially developed in consultation with all operational teams and were modified to incorporate the lessons which were learned during the pre-launch simulation and training exercises. The constraints which guided us to design the orbit acquisition maneuver sequence are:

1. The first maneuver was used to calibrate the 22-N thrusters. This maneuver was in-plane and contributed to the retargeting process. The maneuver magnitude was constrained be between ≈2 m/s and ≈5 m/s.

2. A baseline 7-7-6-6-6-6 maneuver activity timeline was established.

3. The maneuver centroid time was standardized between 10:00 AM and 2:00 PM Pacific Daylight Time (PDT). The time varied within this window to acquire the frozen values for e and ω.

4. The maneuver was constrained to occur during a TDRS view period. The HGA is used for small maneuvers, and the omnis for large maneuvers.

5. Large maneuvers were also constrained by omni-antenna obscuration (due to HGA and GPS antenna blockage) and partial coverage zones.

6. A single backup maneuver was designed for each maneuver to provide quick recovery of the sequence following non-satellite operational delays. The backup was scheduled to occur from three to six days following the nominal maneuver time, and was designed to minimize the length of total orbit acquisition sequence.

7. Do not schedule two maneuvers in the same orbit or within two consecutive orbits due to power and thermal constraints.

8. The last maneuver in the sequence was to provide a smooth transition to the orbit maintenance phase.

9. The remainder of the maneuver sequence was to be redesigned following each maneuver to reflect the observed maneuver performance, actual post-maneuver orbit, and modified error execution model.

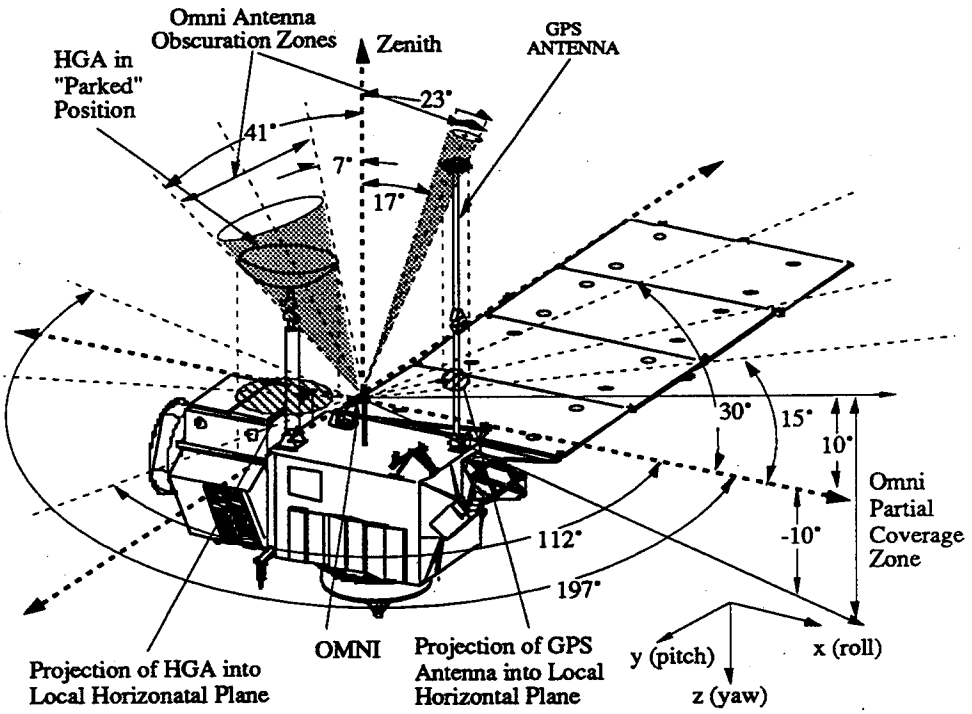

Figure 5. Omnidirectional antenna obscuration.

All satellite communication and control utilize one of the two operational TDRS satellites. During normal operations, the HGA is used for this communication link. The on-board computer (OBC) sends commands to slew the HGA to point toward the correct TDRS and continuously steers the HGA during each TDRS communication. However, it was planned to use the omni antennas during the larger maneuvers which might sufficiently disturb the satellite attitude to interrupt communication. The HGA was thus brought to the parking position (Fig. 5) before every large maneuver. Additionally, the omni antenna may be obscured at times by either the HGA or GPS antennas or booms. During these obscuration periods, the communication link may be lost for a period of time from ≈5 to ≈10 minutes in duration, during which time maneuvers were not permitted.

The communication link was lost a few times during the calibration maneuver because the it was implemented during the omni zone of partial-coverage. The Partial coverage zone is the area between ±10° in elevation with respect to the roll-pitch satellite-fixed plane and forms a circular disc around the satellite. Consequently an additional constraint was imposed during subsequent maneuvers with 22-N thrusters to avoid the partial coverage zone.

MANEUVER DESIGN PROCEDURE

Maneuver sequence design was performed utilizing the Orbit Acquisition Maneuver Software (OAMS). OAMS is derived from GTARG,[13] and incorporates an analytic mean element propagator including perturbations due to Earth oblateness, luni-solar gravity, and impulsive maneuvers. The propagation algorithm utilizes a zonal Earth field to J_{20} and the same recurrence relationships for the geopotential field and luni-solar gravity as GTARG. Maneuver sequence validation was performed with the DPTRAJ precision numerical integration software. DPTRAJ uses a predictor-corrector integrator with automatic step size control and models all known perturbations.[14,15]

OAMS is essentially an analytic orbit propagator which allows for the execution of a single impulsive maneuver which is performed at a specific location (defined in terms of its argument of latitude u) within a particular orbit. The analytic propagation technique allows OAMS to be rapid and efficient yet still reasonably accurate. Its dynamic model includes earth gravity and luni-solar perturbations but ignores drag as its effect (at the TOPEX/POSEIDON altitude) is negligible over the period between successive orbit acquisition maneuvers (six to seven days). Although some consideration was given to including a targeting algorithm, such as a differential correction scheme which iterates on the maneuver sequence, such a tool was not generated due to budgetary constraints. However, the manual iteration required did not prove to be a significant limitation. The rapidity of calculations which may be performed with OAMS allows for the exploration of numerous maneuver alternatives and the design of an entire bootstrapped maneuver sequence in ≈2 to ≈5 hours.

As with GTARG, OAMS takes as its input the standard Keplerian mean elements and then translates them internally to a frame which is non-singular near e ≈ 0, using $\xi = e\cos\omega$, $\eta = e\sin\omega$, and $L = M + \omega$ in place of the usual elements e, ω, and M. Since the objective of the maneuver sequence design was to phase the ground track with the reference grid, OAMS prints a table showing the difference between the actual and reference equatorial crossing longitudes as a function of time (once per orbit). An impulsive maneuver of a desired magnitude and direction is executed at a specified u and the propagation then continues using post-maneuver orbital parameters.

The evolution of the ground track phasing from injection to the operational orbit is represented in terms of the ground track drift rate and the history of ascending node crossing longitudes. The basic in-plane sequence design equation is

$$\lambda_D = d_1(t_1 - t_0) + d_2(t_2 - t_1) + \cdots + d_n(t_n - t_{n-1}) \tag{1}$$

where λ_D is the net equatorial ground track change, d_i is the ground track relative drift rate after maneuver i, and t_i is the time of maneuver i. Changes in the ground track drift rate were accomplished through maneuvers which were implemented at pre-determined times. The actual positioning of the maneuver in the orbit was selected to adjust the eccentricity vector. Given a target reference track the initial value of λ_D was determined. Each maneuver was designed individually and the sequence checked with eq. (1) to verify ground track phasing. Parametric variables for successive iterations of the sequence were (a) selection of the target reference track, (b) the maneuver magnitudes, and (c) the number of maneuvers. Out-of-plane maneuvers were

designed independently. The ground track drift during the out-of-plane maneuvers and the expected in-plane error components due to the out-of-plane maneuvers were also taken into account in designing the rest of the sequence. The result was a minimum duration maneuver sequence phasing the ground track to within ±1 km of the reference.

The in-plane maneuver magnitudes were adaptive in nature. After each maneuver, the remainder of the sequence was redesigned using updated error models and absorbing the execution error of the previous maneuver. Larger maneuvers (> 400 mm/sec) were implemented earlier. A "shoot-short" strategy, in which each maneuver was designed incorporating $\pm 3\sigma$ execution errors so that the resulting ground track would not cross the target reference track prior to the subsequent in-plane maneuver. In this way the ground track approached the target from one direction.

Each sequence was simulated in DPTRAJ after it was designed with OAMS. Finite thrust maneuvers and all force models were utilized by this precision numerical integration. The predicted post-maneuver mean elements and nodal crossings generated by DPTRAJ were used to validate the maneuver design. As OAMS was calibrated with DPTRAJ prior to launch, it was never necessary to modify the maneuver magnitude as a result of this verification procedure. These validated maneuver parameters (ΔV magnitude and maneuver centroid time) are referred to as the *ideal maneuver parameters.*

While the maneuver parameters are determined as an ideal ΔV magnitude and direction, the OBC commands are specified as quantized thruster-on durations. This conversion from the ideal maneuver parameters into the *commandable maneuver parameters* is performed by the Satellite Performance Analysis Team (SPAT). The commandable maneuver duration is then converted back into ΔV units by SPAT and returned to the NAVT. The commandable ΔV magnitude is again verified using DPTRAJ prior to final maneuver implementation approval.

ERROR MODEL

The principal error sources during orbit acquisition maneuver sequence design were injection and maneuver execution errors. Operational orbit determination uncertainties were negligible compared to these errors and hence were neglected during the sequence design.* Once the injection orbit was well determined, only maneuver execution errors were considered for the remainder of the design process. The error model which was used prior to launch[16] is summarized in Table 2.

Although the pre-launch navigational design incorporated pointing errors, these were not considered after launch as they were accounted for in the command implementation process (which is not performed by the NAVT). The first four maneuver were implemented using four 22-N thrusters and the last two using four 1-N thrusters. The errors were dominated by the proportional ΔV error, which is proportional to the maneuver magnitude. The fixed error accounts for quantization errors, thrust ramp-up and repeatability, and other errors which are independent of maneuver duration, and was not changed during the acquisition period. After the first maneuver utilizing the 22-N thrusters, the proportional error was reduced from 10% to 5%, and to 3% for subsequent maneuvers. After the first maneuver using the 1-N thrusters, their proportional errors were also reduced to 3% based on their observed performance.

---

* Due to their high precision, the same can not be said of orbit maintenance maneuvers. For these later maneuvers, maneuver execution, orbit determination, and drag prediction errors are all of comparable magnitude.

Table 2
Pre-launch maneuver execution error model.

	3σ Errors 22-N Thrusters		3σ Errors 1-N Thrusters	
Parameter	1st Maneuver	After 1st Maneuver	1st Maneuver	After 1st Maneuver
ΔV (Proportional)	10%	5%	10%	5%
ΔV (fixed)	16 mm/sec†	16 mm/sec†	0.4 mm/sec**	0.4 mm/sec**
Pointing error (Pitch)	3.5°	2°	3.5°	2°
Pointing error (Yaw)	3.5°	2°	3.5°	2°

MANEUVER PERFORMANCE EVALUATION

Maneuver execution evaluation accuracy requirements, which were determined jointly by the NAVT and FDF, were dictated by the need to phase the ground track with a minimum number of maneuvers. The accuracy requirement is a function of maneuver magnitude and improved accuracy was needed for smaller maneuvers (ΔV < 100 mm/sec). It was determined that such maneuvers required a precision of ±0.2 mm/sec.[4]

Maneuver evaluation is based upon a comparison of pre-maneuver and post-maneuver orbit determination (OD) results. The FDF uses different procedures for evaluating larger (> 100 mm/sec) and smaller (< 100 mm/sec) maneuvers. Pre-maneuver and post-maneuver OD solutions are determined at the epoch of the maneuver centroid. The velocities are then differenced to obtain the maneuver magnitude. The difference between the two methods is that spatially constrained OD solutions are used in evaluating smaller maneuvers. This procedure was verified by simulating a null maneuver (0.0 mm/s) and showing the results to be smaller than 0.2 mm/sec.

A different method is used by the NAVT at JPL. This analytical technique uses pre-maneuver and post-maneuver mean elements[9] at the same epoch. The change in the Keplerian mean elements is a function of maneuver magnitude and direction. By solving for this relationship, the maneuver performance is calculated. Assuming impulsive thrusts, the velocity change can be expressed vectorally as

$$\Delta\bar{V} = \begin{pmatrix} \Delta V_r \\ \Delta V_t \\ \Delta V_c \end{pmatrix} = \begin{pmatrix} F_r \\ F_t \\ F_c \end{pmatrix} \Delta t = \bar{F}\Delta t \qquad (2)$$

where the subscripts r, t, and c refer to the radial, transverse, and normal directions, F is the acceleration and Δt is the thrust duration.

The changes in the mean Keplerian elements due to a maneuver is given by[17]

† Four thruster maneuver.
** Two thruster maneuver.

$$\Delta a = \frac{2}{n}\left[\Delta V_r \frac{e\sin f}{\sqrt{1-e^2}} + \Delta V_t \frac{a}{r}\sqrt{1-e^2}\right] \tag{3}$$

$$\Delta e = \frac{\sqrt{1-e^2}}{na}\left[\Delta V_r \sin f + \Delta V_t \frac{a}{er}\left(1-e^2-\frac{r^2}{a^2}\right)\right] \tag{4}$$

$$\Delta i = \Delta V_c \frac{r\cos u}{na^2\sqrt{1-e^2}} \tag{5}$$

$$\Delta\Omega = \Delta V_c \frac{r\sin u}{na^2\sqrt{1-e^2}\sin i} \tag{6}$$

$$\Delta\omega = -\frac{\sqrt{1-e^2}}{nae}\left[\Delta V_r \cos f - \Delta V_t\left(1+\frac{r}{a}\frac{1}{(1-e^2)}\right)\sin f + \Delta V_c \frac{r}{a}\frac{e\cot i\sin u}{(1-e^2)}\right] \tag{7}$$

$$\Delta M = \frac{(1-e^2)}{nae}\left[\Delta V_r\left(\cos f - \frac{r}{a}\frac{2e}{(1-e^2)}\right) - \Delta V_t\left(1+\frac{r}{a}\frac{1}{(1-e^2)}\right)\sin f\right] \tag{8}$$

where r is the radial distance of the satellite, $u = \omega + f$ is the argument of latitude, and f is the true anomaly. Eqs. (3) through (8) are simplified by assuming a nearly circular orbit ($e << 0.005$) and only keeping terms to first order in e.

$$\Delta a = \frac{2}{n}\left[\Delta V_r e\sin f + \Delta V_t \frac{a}{r}\right] \tag{9}$$

$$\Delta e = \frac{1}{na}\left[\Delta V_r \sin f + \Delta V_t \frac{a}{er}\left(1-\frac{r^2}{a^2}\right)\right] \tag{10}$$

$$\Delta i = \Delta V_c \frac{r\cos u}{na^2} \tag{11}$$

$$\Delta\Omega = \Delta V_c \frac{r\sin u}{na^2\sin i} \tag{12}$$

$$\Delta\omega = -\frac{1}{nae}\left[\Delta V_r \cos f - \Delta V_t\left(1+\frac{r}{a}\right)\sin f + \Delta V_c \frac{r}{a}(e\cot i\sin u)\right] \tag{13}$$

$$\Delta M = \frac{1}{nae}\left[\Delta V_r\left(\cos f - \frac{2re}{a}\right) - \Delta V_t\left(1+\frac{r}{a}\right)\sin f\right] \tag{14}$$

Eqs. (9) and (10) can be combined to give ΔV_t as a function of Δa and Δe, eq. (11) gives ΔV_c as a function of Δi, and eqs. (13) and (14) can be combined to give ΔV_r as a function of $\Delta\omega$, ΔM, and ΔV_c. The result is

$$\Delta V_t = \frac{an}{2r}(\Delta a - 2ae\,\Delta e) \tag{15}$$

$$\Delta V_c = \frac{na^2}{r\cos i}\Delta i \tag{16}$$

$$\Delta V_r = -\frac{na^2}{2r}(\Delta\omega + \Delta M) - \frac{nae}{2}\Delta V_c \sin u\cot i \tag{17}$$

Eqs. (15) through (17) are used for maneuver evaluation. Prior to launch, this procedure was validated by DPTRAJ simulations of finite maneuvers and by comparison with the results of simulations performed by FDF. A typical example is given in Table 3. This example simulates an in-plane two-thruster maneuver ($\Delta V \approx 2.0$ mm/sec) of 2.5 sec duration starting at 02:00:00 UTC on June 16, 1993. Two trajectory files were generated with DPTRAJ, but only one of these files contained the maneuver. All force models were utilized and finite-maneuvers were simulated. States were extracted from both of these files at the same epoch, 02:00:04 UTC (just after maneuver burn-out time). These two states were converted to mean elements representing the pre-maneuver and post-maneuver states. Taking the differences in the mean elements, the components of velocity change were computed using eqs. (15) through (17). The results of all simulations performed matched the FDF results and demonstrated that this technique had a precision better than the required ±0.2 mm/s accuracy in maneuver evaluation.

Table 3.
Typical maneuver simulation as described in the text.

Parameter	Pre-Maneuver Orbit	Post-Maneuver Orbit	Difference
a, km	7714.42635	7714.43064	4.29296×10^{-3}
e	0.0000717	0.0000714	-4.761×10^{-7}
i	66.04195°	66.04195°	-2.489×10^{-9}
Ω	331.43605°	331.43605°	-3.675×10^{-9}
ω	64.84102°	64.50293°	-0.26680
M	229.38652°	229.72461°	0.26680
ΔV, mm/sec	---	---	2.00017

This technique was successfully used during the Orbit Acquisition Phase and better than ±0.2 mm/s accuracy was achieved for all maneuvers including inclination changes. This precise maneuver evaluation helped to minimize the number of maneuvers and to successfully phase the ground track with a smooth transition to the operational phase. The results of the analytic technique agreed closely with the FDF evaluation. For example, the two methods agreed to within 0.04 mm/sec for the TRM maneuver (NAVT ΔV=74.0 mm/sec, FDF ΔV=74.03 mm/sec).

MANEUVER SEQUENCE IMPLEMENTATION

As maneuver implementation was complex detailed operational procedures were instituted to ensure that all activities were performed correctly and in the proper sequence. An initial 5-5-4-4-4- - - activity timeline,* developed in cooperation with all other teams,[11] was found via pre-launch simulation and training exercises to have insufficient spacing between maneuvers for all mission support activities to be completed. Consequently the procedures were revised and a 7-7-6-6-6- - - activity timeline was adopted as the final baseline activity timeline. An operationally feasible 3-day to 6-day delay backup philosophy was also determined to acquire the operational orbit.

* The numbers indicate the spacing in days between consecutive maneuvers. Thus with a 5-5-4-4-4-4 sequence timeline, the first maneuver is performed 5 days after launch, the second maneuver 10 days after launch, and all subsequent maneuvers at 4-day intervals. The total number of maneuvers in the initial design was seven rather than six to allow for an additional inclination trim maneuver, which was not required. The initial timeline required that all maneuvers be performed 3:00 PM PDT (±1 orbit); with the final timeline this was revised to 12:00 Noon (±1 orbit).

Prior to launch, the baseline sequence was designed incorporating the best-known pre-launch maneuver execution estimates[16] and an injection error model which was based upon data provided by Ariane.[18] The baseline sequence had seven maneuvers including calibration, inclination, and inclination trim maneuvers (Fig. 6). The number of maneuvers in the sequence is a function of the size of injection and execution errors.[11] Potentially large injection inclination errors and simulated attitude pointing errors were projected and incorporated into this baseline design. The inclination-trim maneuver was included to remove any residual inclination errors which resulted from the other maneuvers. The sequence design was consistent with all operational constraints and met all requirements. It correctly phased the ground track and achieved the frozen orbit in 44 days. A "shoot-short" strategy was applied to avoid a penalty in terms of extra days required to achieve the operational orbit under the expected worst-case execution errors.

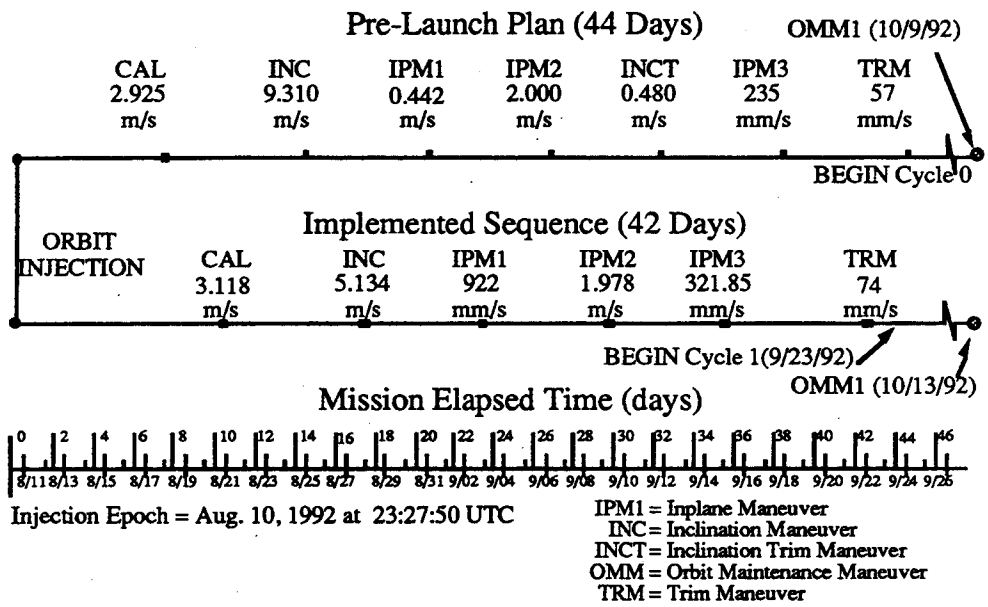

Figure 6. Maneuver sequence design and execution.

After launch, the maneuver sequence was re-designed using the achieved injection orbit and the pre-launch execution error model. The achieved inclination was 41 mdeg higher than the operational orbit inclination, and required $\Delta V \approx 5.2$ m/s for correction, approximately one-half of the inclination change allowed for in the baseline design. Pointing errors were neglected during maneuver design, but were accounted during the command implementation process. Actual pointing errors ($<<1°$) were much lower than the expected worst case pointing errors of 3.5° (Table 2). The inclination-trim maneuver became unnecessary because of the low injection errors imparted by the launch vehicle and the extremely low pointing errors. The updated sequence required only six maneuvers and would have reached the operational orbit in 38 days.

Primary and back-up sequences were designed for each maneuver. Operational constraints require the scheduling of the back-up maneuver with a delay of between three and six days and the remaining maneuvers in the sequence at the same spacing as originally planned (Fig. 7). It only became necessary to delay a maneuver once. Due to a time correlation inconsistency between the satellite and the ground segment, the first maneuver was delayed approximately 3 days. The rest of the sequence proceeded along a 10-7-6-6-6-7 timeline.

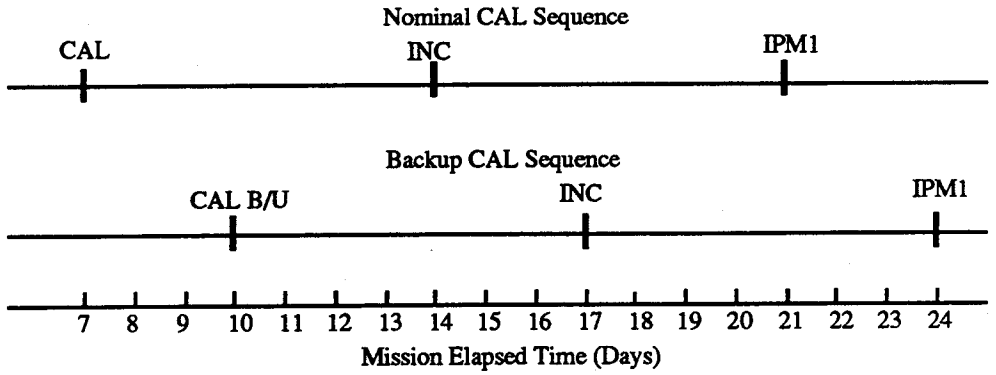

Figure 7. Scheduling a delayed maneuver.

All maneuver designs were adaptive to last-moment adjustments in the maneuver centroid times. These shifts occurred to avoid unexpected operational problems, principally due to changes in TDRS coverage, usually due to the emergency coverage requirements of other satellites or to support STS landing operations. For example, the centroid of maneuver IPM1 was moved nearly 17° (Figure 8) to adapt to changes in TDRS coverage, resulting in poor targeting of the eccentricity vector (e, ω). However, the target eccentricity vector was achieved by the modification of subsequent maneuvers. Changes required in the other maneuvers were minor were easily adapted to.

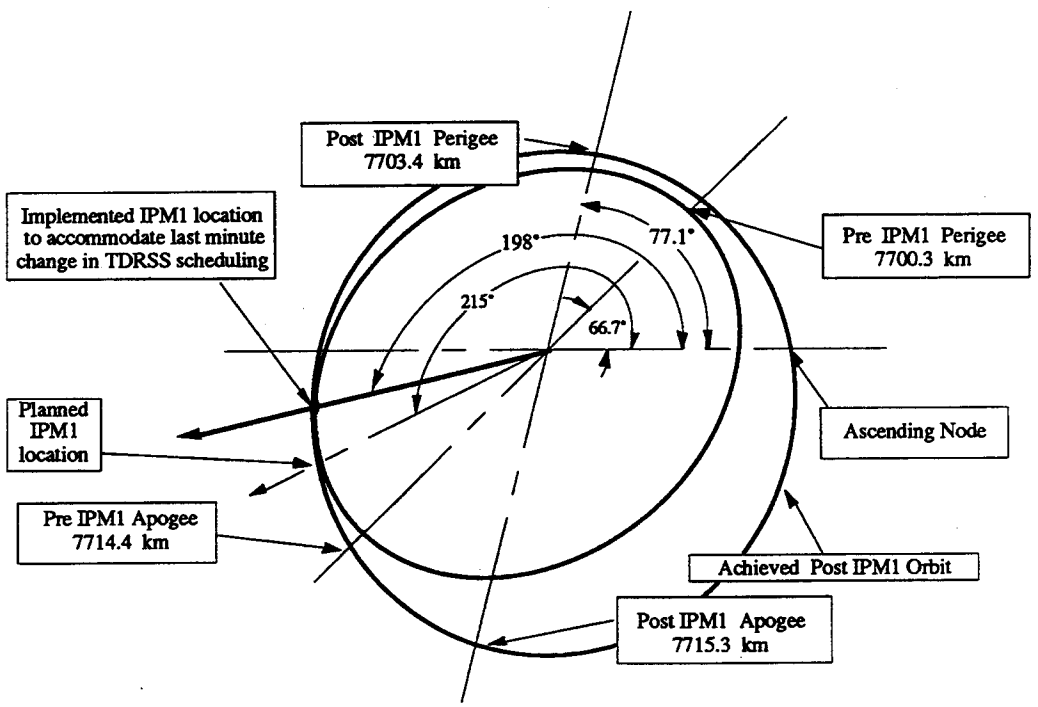

Figure 8. Last moment change in In-Plane Maneuver 1 (IPM1) implementation.

RESULTS

Due to the low level of injection errors actually achieved and the highly accurate and repeatable levels of thrust provided by the on-board propulsion system, the orbit acquisition maneuver sequence was completed two days sooner and with one fewer maneuvers than planned (after only 42 days). This was despite the fact than the first maneuver was delayed three days, the corresponding backup sequence performed, and conservative execution error estimates were used for the sequence design although satellite performance was excellent. Subsequent to the completion of the maneuver sequence satellite operations made a smooth transition to the orbit maintenance phase.

The implemented sequence contained six maneuvers and reached the operational orbit in 42 days (Fig. 9(a)). The calibration maneuver (CAL) was implemented on 10th day of the mission. The four large maneuvers using 22-N thrusters were completed by in-plane maneuver 2 (IPM2) in 29 days utilizing a 10-7-6-6 timeline. The first maneuver (CAL) was performed primarily to calibrate the four 22-N thrusters and secondarily to raise the orbit. The ideal maneuver CAL magnitude was 3000.00 mm/s and the corresponding commandable maneuver magnitude was 3002.03 mm/s (Table 4). Maneuver performance was nearly 4% higher than expected. The second maneuver consisted of an out-of-plane inclination change maneuver (INC) which almost completely removed the inclination error imparted by the launch vehicle. Performance was better than expected (-1.2%) thereby eliminating the need for an inclination trim maneuver. The performances of in-plane maneuver 1 (IPM1) and in-plane maneuver 2 (IPM2) were better than one percent. Pointing errors were significantly smaller than expected (<<1°), because the thrusters were precisely calibrated and the center of thrust was extremely well aligned with the center of mass.

Table 4
Summary of Maneuver Performance. All ΔV's are expressed in mm/sec and utilized four thrusters.

Maneuver.	Date (1992)	Thrusters	Ideal ΔV	Commanded ΔV	Achieved ΔV	Error
CAL	Aug. 20	22-N	3000.00	3002.03	3118.75	+3.9%
INC	Aug. 27	22-N	5200.00	5195.42	5134.14	-1. 2%
IPM1	Sept. 2	22-N	920.00	919.87	921.68	+0.2
IPM2	Sept. 8	22-N	1980.00	1979.75	1978.62	-0.1%
IPM3	Sept. 14	1-N	320.00	319.97	321.85	+0.6%
TRM	Sept. 21	1-N	74.00	74.03	74.00	nil

In-plane maneuver 3 (IPM3) was the first maneuver to be implemented using 1-N thrusters. The pre-launch error model was used to design IPM3. Maneuver results were excellent, with better than one percent errors, proving the baseline error model to be overly conservative (Table 4). The resulting ground track drift rate was 1.4 km/day, which was slightly smaller than required to perform the trim maneuver (TRM) six days later, and consequently the TRM was performed seven days after IPM3. The performance of the TRM was excellent and the error was almost nil. The acquisition sequence was completed following the TRM on September 21, 1992, 42 days after launch, with the satellite in the operational orbit and the ground track phased with the reference.

The ground track phasing process is shown in Fig. 9(b). The large maneuvers (ΔV > 400 mm/sec) which used the 22-N thrusters reduced the drift rate from ≈108.08 km/day to ≈6.7 km/day. The drift rate after IPM3 was ≈1.4 km/day and was lower than expected. The TRM maneuver reduced the drift rate to nearly zero (≈136 m/day). The TRM maneuver was designed

so that the post maneuver drift rate would provide a smooth transition to the orbit maintenance phase, with the first ground track maintenance maneuver (OMM1) to be performed on Oct. 13, 1992.

The single out-of-plane maneuver did not contribute to raising the orbit or phasing the ground track. Its purpose was to remove the inclination error imparted by the launch vehicle. All in-plane maneuvers contributed to raising the semi-major axis (Fig. 9c) and to achieve the frozen orbit (Fig. 10). The orbit was nearly operational by IPM2 but both IPM3 and TRM were required to refine the semi-major axis and the eccentricity vector, and to bring the ground track within the control band. The achieved orbit after the TRM maneuver met all tolerance requirements, as shown in table 5.

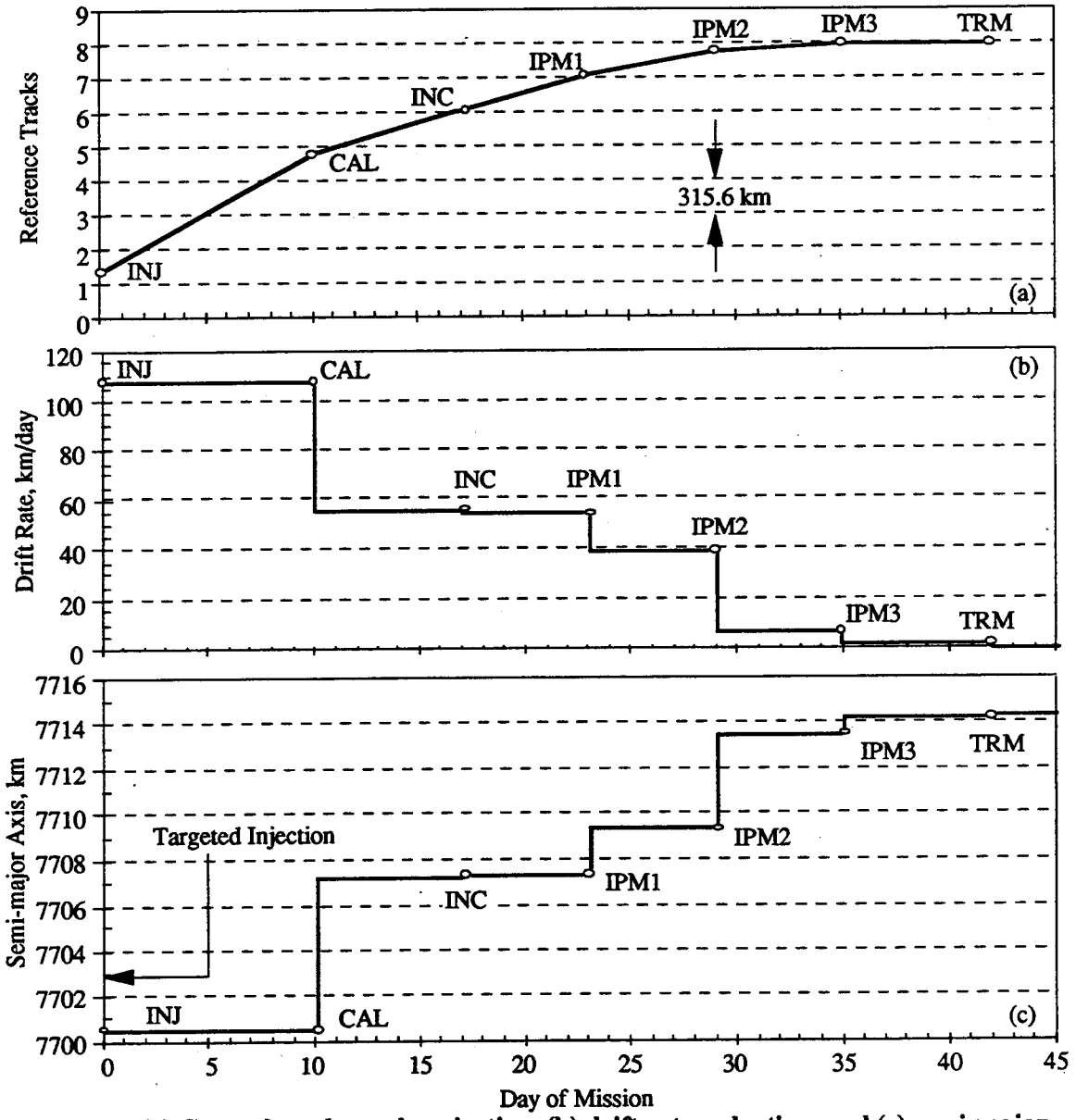

Figure 9. (a) Ground track synchronization, (b) drift rate reduction, and (c) semi-major axis history.

The ground track following the TRM maneuver was ≈1.65 km west of the reference and drifting slowly eastward, at ≈136 m/day as illustrated in Fig. 11. It entered the control band and was approaching the eastern edge by the transition between repeat cycles 2 and 3, providing a smooth transition to the orbit maintenance phase. Orbit maintenance maneuver 1 (OMM1) was performed on Oct. 13, 1992.

Table 5.
Achieved orbit at the end of the orbit acquisition maneuver sequence.

Mean Element	Reference Value	Tolerance	Achieved Value	Difference
a, km	7714.429	---	7714.412	- 0.017
$e \times 10^{-6}$	95	±50	137	42
ω	90.0°	±15.0°	92.3°	2.3°
i^*	66.040°	±0.003°	66.041°	0.001°

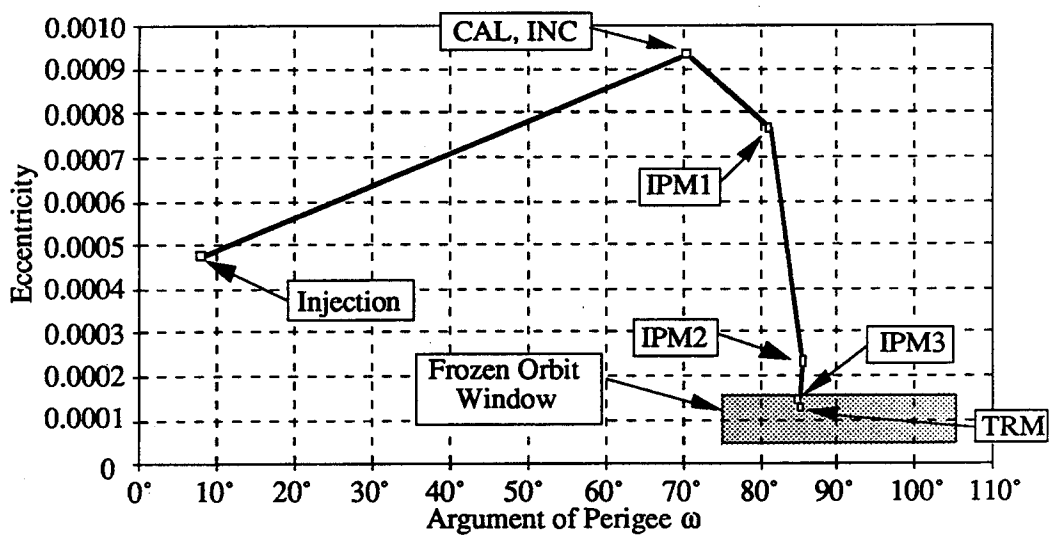

Figure 10. Acquisition of the frozen orbit.

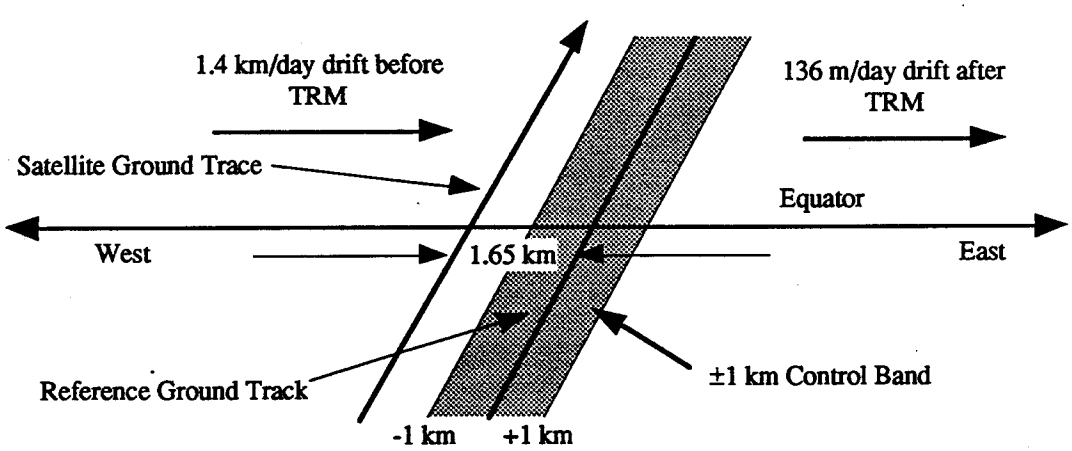

Figure 11. Ground track at the end of the orbit acquisition maneuver sequence.

* Gravity mean inclination.

CONCLUSIONS

The TOPEX/POSEIDON acquisition maneuver sequence was completed in 42 days. This process removed injection errors, raised the orbit, and decreased the eccentricity to reach the operational orbit while phasing the ground track to within ±1 km of the reference. The acquisition period was extended by three days due to operational delays in implementing the first maneuver. The inclination trim maneuver was unnecessary due to the small maneuver execution errors. A new maneuver evaluation technique was developed, validated, and used during the orbit acquisition phase. Maneuvers were evaluated to a precision of better than 0.2 mm/sec. Satellite performance was excellent throughout due to precise calibration of thrusters. While a conservative error model was used throughout, a much tighter error budget could have been permitted and this would have eliminated one maneuver. Pointing errors were significantly smaller than expected (<< 1.0°) even though open loop firing tables were not utilized.

The orbit acquisition maneuver sequence required six maneuvers. These included one for calibration, one out-of-plane maneuver to correct the inclination, and four additional in-plane maneuvers to raise the semi-major axis, decrease the eccentricity, rotate the line of apsides, and phase the ground track. All maneuvers were performed at logistically convenient times during normal working hours. The sequence implemented corresponded to a 10-7-6-6-6-7 timeline and was robust enough to respond to new calibration factors and scheduling changes in a timely fashion without operational delays. All operational requirements were met and no constraints were violated. After the sequence was completed, a smooth transition was made to the orbit maintenance phase.

ACKNOWLEDGEMENTS

Tom Hamilton provided many useful suggestions during the orbit acquisition process. Jerome Teles, Ed Doll and the FDF operations and contractor staff provided a steady stream of OD results and analyses at all hours of the day, and considerably smoothed inter-agency communications. Thanks are due to A. R. Zieger and T. A. Adamski for their encouragement throughout the course of this work.

REFERENCES

[1]Carlisle, George, A. Dicco, H. Harris, A. Salama, M. Vincent, *TOPEX/POSEIDON Project Mission Plan*, Jet Propulsion Laboratory, JPL D-6282, rev. C., Aug. 1991 (Internal Document).

[2]Vincent, M.A, *TOPEX/POSEIDON Orbit Characteristics*, Jet Propulsion Laboratory, JPL D-7511, June 1990 (Internal Document).

[3]TOPEX/POSEIDON Project, *Mission and Systems Requirements*, Jet Propulsion Laboratory, JPL D-5901, April 1989 (Internal Document).

[4]Goddard Space Flight Center Flight Dynamics Facility, *TOPEX/POSEIDON Interface Control Document*, 554-FDD-91/116, June 1992.

[5]Vincent, M.A., "The Inclusion of Higher Degree and Order Gravity Terms in the Design of a Repeat Ground Track," AIAA-90-2899-CP, *AIAA/AAS Astrodynamics Conference*, Portland, Oregon, Aug. 1990.

[6]Marsh, J.G., et. al., *The GEM-T2 Gravitational Model*, NASA Technical Memorandum 100746, Oct. 1989.

[7]Shapiro, B. E., *TOPEX/POSEIDON Repeat Orbit and Reference Grid Definition* Jet Propulsion Laboratory JPL IOM No. 314.5 - 1642, June 22, 1992 (Internal Document).

[8]Lerch, F.J., et. al., *Geopotential Models of the Earth from Satellite Tracking, Altimeter and Surface Gravity Measurements: GEM-T3, GEM-T3S*, NASA Technical Memorandum 104555, Jan. 1992.

[9]Guinn, J.R., "Short-Periodic Gravitational Perturbations for Conversions between Osculating and Mean Elements," AAS 91-430, *AAS/AIAA Astrodynamics Conference*, Durango, Colorado, Aug. 19-22, 1991.

[10]Bhat, R. S., *Execution Error Model for Orbit Maintenance Maneuver Design*, Jet Propulsion Laboratory IOM FOS 92-034, Oct. 2, 1992 (Internal Document).

[11]Bhat, R. S., "TOPEX/POSEIDON Orbit Acquisition Maneuver Design," AAS 91-514, *AAS/AIAA Astrodynamics Specialist Conference*, Durango, Colorado ,Aug. 19-22, 1991.

[12]Sanneman, P., *TOPEX/POSEIDON Orbit Adjust Mode Impact of CM Estimation Uncertainty and ACS Thruster Failures on ΔV Maneuver Performance*, Fairchild Space Company, GNC:TOPEX90-079, June 1990.

[13]Shapiro, B. E. and Bhat, R.S., "GTARG - The TOPEX/POSEIDON Ground Track Maintenance Maneuver Targeting Program," *AIAA/AHS/ASEE Aerospace Design Conference*, AIAA 93-1129, Feb. 16-19, 1993, Irvine, CA.

[14]Ekelund, J.E., Sunseri, R. F., and Collier, J.B., *DPTRAJ/ODP User's Reference Manual*, Jet Propulsion Laboratory, JPL D-263, Oct. 1991 (Internal Document).

[15]Spier, Gerd W., *Design and Implementation of Models for the Double Precision Targeting Program (DPTRAJ)*, Jet Propulsion Laboratory, Technical Memorandum 33-451, April 15, 1971 (Internal Document).

[16]Frauenholz, R.B. and Hill, M.H., Maneuver Execution Errors for the Pre-launch Assessment Phase Maneuver Design, Jet Propulsion Laboratory, IOM FOS-92-348, June 16, 1992 (Internal Document).

[17]Meirovitch, Leonard, *Methods of Analytical Dynamics*, New York: Mc Graw Hill, 1970.

[18]Carlisle, G.L., *Mission Target Specification (Final)*, Jet Propulsion Laboratory TOPEX/POSEIDON Project 633-334, Rev. C, Oct. 1991 (Internal Document).